

# IDENTIFICATION OF FAULT CONTINUITY AND HOT WATER RESERVOIR USE SCHLUMBERGER CONFIGURATION RESISTIVITY METHOD IN CANGAR

Dhony Widyasandy<sup>1\*</sup>, Aulia K Nugraha<sup>2</sup>, Husni Cahyadi Kurniawan<sup>3</sup>, Ahmad Luthfin<sup>4</sup>

<sup>1</sup>*Department of Physics, Sultan Maulana Hasanuddin Islamic University of Banten*

<sup>2</sup>*Brawijaya Volcano and Geothermal Research Center, Brawijaya University*

<sup>3</sup>*Department of Physics Education, State Islamic Institute of Tulungagung*

<sup>4</sup>*Department of Physics, Universitas Islam Negeri Maulana Malik Ibrahim Malang*

*Received: 17<sup>th</sup> December 2019; Revised: 10<sup>th</sup> February 2020; Accepted: 17<sup>st</sup> September 2020*

## ABSTRACT

Research that uses the Schlumberger configuration resistivity method had been conducted in Cangar. The purpose of this study is to identify cracks/faults and potential hot springs use resistivity well analysis and correlate it with rock lithology in Cangar, East Java. Data acquisition is carried out using 3 tracks with 10 sounding points. The space between points is 50 meters. The rock resistivity values obtained were 9945  $\Omega\text{m}$ , 7360  $\Omega\text{m}$ , and 5573  $\Omega\text{m}$  which were thought to be breccia layers and functioned as hot springs. This estimation is strengthened by the existence of a layer of breccia-andesite because this layer is very good as a water reservoir. In addition, based on the lateral cross-section on lane 1, there was a decrease in boulder-sized breccia-andesite layers; this decrease was the production of faults.

**Keywords:** Geothermal; Schlumberger Configuration; Resistivity; Lateral Cross-section.

## Introduction

Geothermal is a natural phenomenon that can be found in Cangar area of Sumber Brantas Village, Bumi Aji District, Batu City. The geothermal symptom is characterized by manifestations including hot springs and hot spring pools on the west side of Welirang Mountain. The source of hot spring is estimated to come from volcanic rocks that experience fault under the cone of Arjuno-Welirang Mountain and has a function as reservoir rocks. This volcanic rock is impermeable that has a function as a hood.

Manifestations of geothermal in Cangar hot springs have been studied by many researchers. Previous research has been carried out referring to a purpose; the identification of geothermal sources in the area. Based on the results of the magnetotelluric study that is conducted by the Center for Geological Resources<sup>1</sup> a low resistivity anomaly related to the caprock appears beneath Arjuno-Welirang Mountain

to the northwest area. The heat source will heat the fluid stored in a reservoir that is covered by cap rock. This manifestation of hot water appears in Coban, Cangar, and Padusan which represent the outflow zone in the Arjuno-Welirang mountain geothermal system.

According to Rakhmanto<sup>2</sup> his study entitled Geo-electric Tomography Cangar Hot Springs explained that there were faults in the south of the baths. Faults were in the lava rock layers that indicate fluid flow in the form of water from the source. Affandi<sup>3</sup> had also conducted a study that used magnetic methods with extensive research areas ranging from Cangar hot springs to Sumber Brantas Village with the results of residual anomaly contours to -1000 nT values, it was located in the North and West of the manifestation of hot water. The magnetized volcanic rocks and geothermal potential in that position had a susceptibility value of -3,166 which has a volume of  $\pm 1,550,345 \text{ m}^3$  and a susceptibility of -0,018 which has a volume of  $\pm 16,610 \text{ m}^3$ .

\*Corresponding author.

E-Mail: dhony.widyasandy@gmail.com

Next Previous studies Dafiqiy<sup>4</sup> based on the results of studies that had been presented in his research used the self-potential method in Cangar area, the potential distribution value of the potential map could be predicted that the system of hot fluid flow from the southeast to the northwest.

This study used the Schlumberger configuration resistivity geoelectric method. The selection of this method was based on technical considerations related to target penetration that can reach a depth of 50 m. Another consideration was that the Cangar Region is an environmental conservation area. With the theme “Identification of Fault Continuity and Hot Water Reservoir use Schlumberger Configuration Resistivity Method in Cangar”, it is expected to provide accurate information in the form of good data about lithology at the measuring point and its depth data.

**Methods**

Data was collected in Cangar Hot Springs and R. Soeryo Forest Park, Sumber Brantas Village, Bumi Aji District, Batu City. The geophysical method in this study is the resistivity method with the Schlumberger configuration. The Schlumberger points will be placed evenly in the measurement area according to references in both geological studies that indicate faults and geophysics.

The measuring instrument used in this study was the OYYO Resistivity Meter MCOHM-EL Model-2119D type. This instrument is equipped with 4 electrodes and 4 cable windings. In addition to the primary measuring instrument, this resistivity method measurement can be used if equipped with a Roll-meter, handheld GPS, Hammer, Multimeter, and equipment to record. If the instruments have been equipped, then data acquisition for Schlumberger configuration resistivity in the study area can be carried out.<sup>5</sup>

The assessment path is determined based on the desired interpretation design by considering the natural conditions of the study area. The sounding point is attempted to be measured with a stretch of the electrode in the same direction to facilitate the process of

correlating and facilitate the interpretation of each sounding point, so the measurement between sounding points making it possible to spread the electrodes in the same direction.

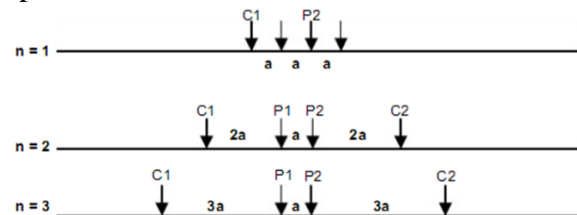


**Figure 1.** Acquisition Model Schlumberger Configuration Data<sup>6</sup>

The data acquisition of resistivity with the Schlumberger configuration is generally described in Figure 1. The position of the potential difference electrodes is placed in the middle of the current electrode. The spacing or distance between current electrodes with a potential difference is  $n$  times the distance of the two potential difference electrodes ( $a$ ). Measurements will be carried out are by shifting the current electrode so far until the distance of the current electrode space is equal to the depth of the identified target.

The survey design and Schlumberger measurement points are shown in Figure 2. The figure provides information that the white lines are the lines of the measurement plan, while the red lines with yellow points are the lines and measurement points after the acquisition. The results obtained from the acquisition are 10 sounding points spread over 3 tracks. Space between points that had been done was 50 m.

Data had been taken depended on weather conditions. Natural conditions determined the direction of the stretch that may be carried out for data collection at the time of measurement. While weather conditions affect the level of soil wetness so it potentially changes the distribution of electric current at the time of measurement. The wet ground surface will be a good conductor of electricity so the electric current will be widely distributed at the surface and less distributed at far depths soil. It will also increase the conductivity of surface rocks so the impact is increasing the measured current exceeds its maximum capability of  $\pm 20$  mA.



**Figure 2.** Resistivity measurement points (yellow point) with the measurement flow (red line)

Data from the acquisition results must be valid and checked again before the researcher starts data processing. After the data is declared good invalidity, the next step is data processing. The principle of processing the resistivity data is to calculate the value of rock resistivity and its distribution in one dimension with medium apparent resistivity.

$$\rho = K \frac{\Delta V}{I} \tag{1}$$

Where,

$\rho$  : Measured resistivity (apparent resistivity)

$\Delta V$  : Measured potential difference

$I$  : Injection current

$K$  : Geometry factor ( $K = n(n + 1)\pi a$  with  $n = 1, 2, 3, 4, 5$  etc)

The next process of data processing results is to analyze or interpret the data quantitatively by looking at the comparability of the resistivity value with the reference resistivity range, so the researcher knows the contrast of measured rock resistivity and the depth of the estimation quantitatively. In

addition to quantitative methods, qualitative methods are also used by comparing quantitative results with stratigraphic or patterns of geological events in the measurement area.

### Result and Discussion

The data from the field was processed with excel software to calculate the value of  $\rho$  and IP2Win software to get the true resistivity value at each sounding point. This is data that uses IP2WIN software:

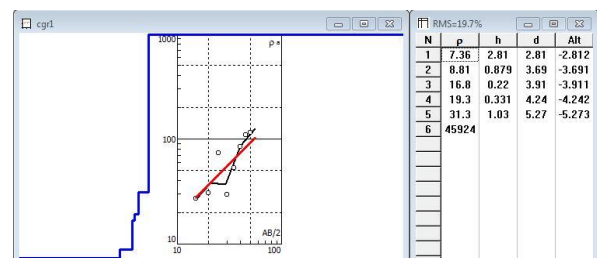


**Figure 3.** Example of processing CGR-1 data uses IP2Win

Generally, the results of manual calculations give suboptimal results and it seems that the error rate is generally 19.7 %. The computer program (IP2Win) then corrects the combination of thickness and true resistivity values to get the smallest number of errors (RMS errors) after several iterations have occurred. The smallest error rate depends on the quality of the field data and the number of parameters entered. If the calculation result still shows a relatively large error value, it will be tried by increasing or decreasing the number of parameters entered and the calculation process starts again.

According to Telford<sup>7</sup> the flow of electric current in rocks can be classified into three types because of the high water that is trapped in the pores of the rock, namely:

1. Electronic conduction if it has free electrons so an electric current is flowed by free electrons.
2. Electrolyte conduction occurs when porous rocks and pores are filled with an electrolyte fluid. In this conduction, the electric current is transferred by electrolytes.
3. Dielectric conduction occurs if there is a dielectric to the flow of electric current that occurs in polarization when the material is electrified.

Technically, the relationship between resistivity and rock type can be concluded as:

1. The porous rock resistivity value is lower than compact rocks.
2. The resistivity value will be lower if the groundwater is high in salt.
3. There is no clear boundary between the resistivity values for each rock.
4. The rock resistivity can be different from one layer to another.
5. Porous rocks that contain water, rock resistivity value are lower than dry rocks and does not contain water. The water content in the rock will indicate the resistivity value of the rock.

Table 2 is a table of resistivity prices range ( $\Omega m$ ) based on Table 1 with reference to Waluyo, 2001. This table interprets the processed geo-electric data to produce lithological estimates, the depth, and

thickness of each layer is described in the table of geo-electric data interpreting results. The data that are obtained have a price of resistivity between 8.56 - 16360.66  $\Omega m$ . The results of data processing in the form of resistivity well data are interpreted quantitatively and qualitatively.

The rock permeability is the ability of the rock to be able to continue the flow of fluid that flows through it and it is usually called a permeable layer. The rocks that are classified as permeable are sandstone and limestone; it is caused by the large inter-grain space so, both are good aquifers. While the impermeable rock layers are clay and shale which have functioned as confining beds.<sup>8</sup> Other factors that affect permeability are hydrostatic pressure, cross-sectional size, and fluid viscosity. Permeability is closely related to the porosity of rocks. Determining porosity uses a comparison of the percentage between the volumes of all stones with the volume of available empty space. The value of porosity is in the range of 10 - 45

**Table 1.** Rock Resistivity Value<sup>5</sup>

Kind of materials	Resistivity ( $\Omega m$ )
Water surface	80 – 200
Groundwater	30 – 100
Silt-clay layer	10 – 200
Sand layer	100 – 600
Sand and gravel layer	100 – 1000
Slime rock	20 – 200
Sandstone	50 – 500
Conglomerate	100 – 500
Tuff	20 – 200
Andesite group	100 – 2000
Granite group	1000 – 10000
Chart group and slate	200 – 2000

**Table 2.** Price range for resistivity type<sup>5</sup>

Resistivity ( $\Omega m$ )	Estimated Lithology
13 – 20	Smooth/Weathered Tuff-Rough
20 – 100	Breccia-Andesite
101 – 200	Andesite
201 – 1000	Solid Andesite

**Table 3.** Resistivity well data correlation result of CGR-1 through CGR-10 with rocks lithology in Cangar<sup>5</sup>

Points	Interpretation Results		Lithology	Thickness (m)
	Depth (m)	Resistivity ( $\Omega\text{m}$ )		
CGR-1	0 – 2,81	7,365	Weathered Tuff	2,81
	2,81 – 3,69	8,811	Solid-Weathered Tuff	0,879
	3,69 – 3,91	16,82	Breccia-gravel andesite	0,22
	3,91 – 4,24	19,31	Breccia-gravel andesite	0,331
	4,24 – 5,27	31,3	Breccia-andesit boulder	1,03
CGR-2	0 – 2,36	11,6	Weathered hard tuff	2,63
	2,63 – 4,12	22,3	Breccia-gravel andesite	1,49
	4,12 – 6,44	65,4	Breccia-andesite boulder	2,32
	6,44 – 8,49	99,4	Andesite	2,05
CGR-3	0 – 0,828	699	Andesite	0,828
	0,828 – 1,69	459	Andesite	0,826
	1,69 – 3,81	547	Andesite	2,12
	7,13 – 8,88	9945	Solid Andesite	1,75
CGR-4	0 – 1,43	10,5	Weathered hard tuff	1,43
	1,43 – 3,43	9,01	Weathered hard tuff	2
	3,43 – 4,9	13,6	Weathered hard tuff	1,47
	4,9 – 6,52	74,2	Breccia-andesite boulder	1,62
	6,52 – 13,1	142	Andesite	6,57
CGR-5	0 – 1,25	34,1	Breccia-gravel andesite	1,25
	1,25 – 4,19	59,2	Breccia-andesite boulder	2,94
	4,19 – 4,44	1,45	Breccia-andesite boulder	0,242
	4,44 – 4,72	4,39	Breccia-andesite boulder	0,289
	4,72 – 14,2	216	Andesite	9,49
CGR-6	0 – 2,95	35,6	Breccia-andesite boulder	2,95
	2,95 – 3,19	43,5	Breccia-andesite boulder	0,239
	3,19 – 3,49	62,1	Breccia-andesite boulder	0,297
	3,49 – 4,23	89,4	Andesite	0,746
	4,23 – 4,79	186	Andesite	0,554
CGR-7	0 – 2,04	9738	Solid andesite	2,04
	2,04 – 3,42	1677	Solid andesite	1,38
	3,42 – 4,45	63,6	Breccia-andesite boulder	1,03
	4,45 – 6,8	63,2	Breccia-andesite boulder	2,34
	6,8 – 9,84	73	Breccia-andesite boulder	3,04
CGR-8	0 – 6,83	7360	Solid andesite	6,83
	6,83 – 12,4	537	Andesite	5,55
CGR-9	0 – 1,97	113	Andesite	0,786
	1,97 – 2,77	143	Andesite	1,18
	2,77 – 3,28	392	Andesite	0,807
	3,28 – 6,33	5573	Solid andesite	3,05
CGR-10	0 – 1,24	10,7	Solid weathered tuff	1,24
	1,24 – 3,38	11,8	Solid weathered tuff	2,15
	3,38 – 3,56	14,7	Solid weathered tuff	0,178
	3,56 – 4,27	22	Breccia-gravel andesite	0,705
	4,27 – 5,28	47,2	Breccia-gravel andesite	1,02

Based on lateral cross-section (Table 3) that is represented by points CGR-1 to CGR-10 shows varying rock layers. CGR-1, CGR-2, CGR-4, CGR-5 and CGR-6 points are located on one track have characteristics that are almost similar only different in their

lithological depth and thickness. If the resistivity wells of each point are aligned, it will give a rough picture of the alternation of rock layers between one point and another in a path.

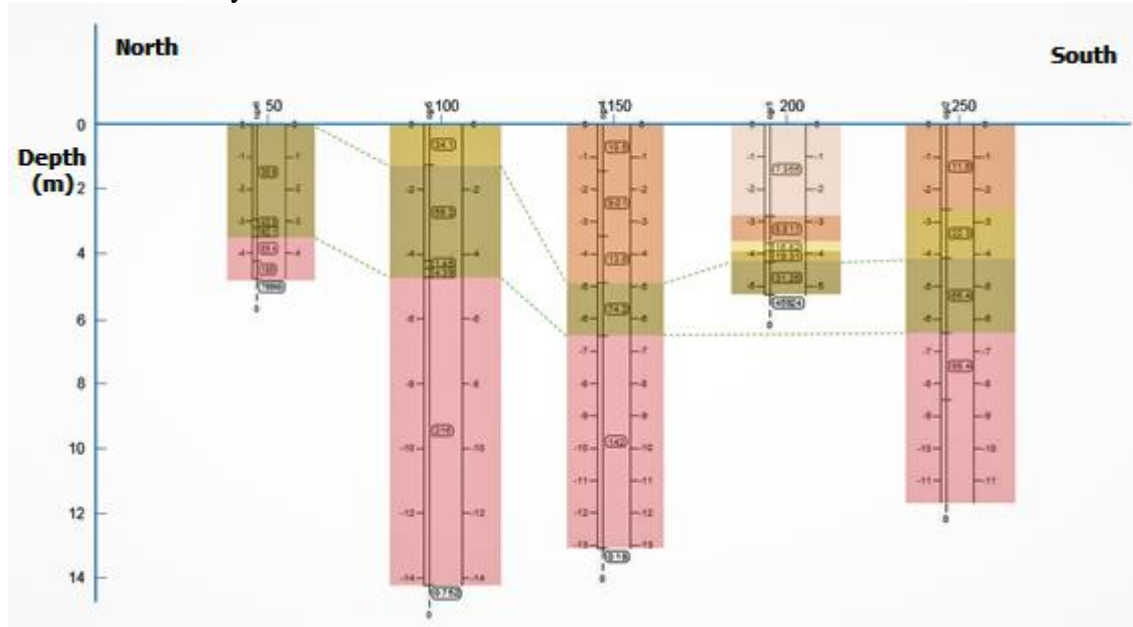


**Figure 4.** Cross-section 1 with resistivity wells CGR-1, CGR-2, CGR-4, CGR-5, CGR-6 which has been correlated with Cangar volcanic rock lithology. The dotted line shows a decreasing layer of breccia-andesite as an indication of faults.

Shown in Figure 4 is a lateral cross-section of the 5 points on track 1. Based on this cross-section image, if it is viewed from the North to South direction there is a decrease in the boulder-sized breccia-andesite layers at the CGR-4, CGR-1 and CGR-2 points. This decrease is the production of faults; based on the topography these points are located across the river that divides track 1.

The type of fault that applies to the track can be concluded as a normal fault. This fault is assumed to have occurred due to the ancient Welirang volcanic activity which is formed the Brantas fault which is in the East of the study site and extends to the South. When the fracture is formed, it indirectly affects the vulnerability of the soil and rock layers below the surface and forms fractures around it, and decreases the surface of the soil.

Besides, the breccia layer on this track has the size of a pebble-gravel so it is very good as a water reservoir because it has a large

porosity. Usually, lump-sized breccia is filled with breccia rocks with smaller porosity as permeable layers and there are weathered layers that have a function as impermeable layers. If it is in an area that has geothermal potential, this breccia will have a function as a hood of the geothermal reservoir layer.

### Conclusions

Based on the results of the study above, it can be concluded that the breccia layer that functions as the place of hot springs was suspected to be found at 3 points from 10 points identified. Firstly, CGR-3 point with rock resistivity of 9945  $\Omega\text{m}$  at a depth of 7.13 - 8.88 m which had a thickness of 1.75 m. Second, the CGR-8 point with 7360  $\Omega\text{m}$  rock resistivity at a depth of 0 - 6.83 m which had a thickness of 6.83 m. Third, CGR-9 point with rock resistivity 5573  $\Omega\text{m}$  at a depth of 3.28 - 6.33 m which had a thickness of 3.05 m. Lateral cross-section at track 1 which was

directed from north to south showed a decrease in boulder-andesite-sized breccia (lump) layers, this decrease was the production of faults. With the layer of breccia-andesite, it was very good as a water reservoir because it had a high porosity.

## References

1. Potensi Panas Bumi di Indonesia Jilid 1. Jakarta: Direktorat Panas Bumi, Direktorat Jenderal Energi Baru Terbarukan dan Konservasi Energi, Kementerian ESDM; 2017.
2. Arjuno-welirang K, Rakhmanto F, Maryanto S, Susilo A. Tomografi Geolistrik Daerah Sumber Air Panas Cangar, Batu. 2011;1(2).
3. Afandi A, Maryanto S, Susilo A. Survei Geomagnetik di Daerah Cangar, Kota Batu, Jawa Timur untuk Mengkaji Potensi Panasbumi. Nat B. 2012;1(3):287–95.
4. Nuha DYU, Maryanto S, Santoso DR. Determination of the Direction of Hot Fluid Flow in Cangar Area, Arjuno-Welirang Volcano Complex, East Java Using Self Potential Method. J Penelit Fis dan Apl. 2017;7(2):123.
5. Waluyo. Panduan Workshop Eksplorasi Geofisika (Teori dan Aplikasi) Metode Resistivitas. Laboratorium Geofisika Universitas Gadjahmada; 2001.
6. Patra HP, Nath SK. Schlumberger Geoelectric Sounding in Ground Water: Principle, Interpretation, and Application. Rotterdam: A.A. Balkema; 1999.
7. Telford WM, Geldart LP, Sheriff RE. Applied Geophysics: Second Edition. 2nd ed. Cambridge: Cambridge University Press; 1990. 770 p.
8. Sosrodarsono, Takeda. Hidrologi Untuk Pengairan. Jakarta: Pradnya Paramita; 1976.